Environmental Earth Sciences (2018) 77:54
https://doi.org/10.1007/s12665-017-7217-1

ORIGINAL ARTICLE

Influence of diversion channel section type on landslide dam draining effect

Tianlong Zhao[1] · Shengshui Chen[2] · Changjing Fu[1] · Qiming Zhong[3]

Received: 19 July 2017 / Accepted: 29 December 2017 / Published online: 20 January 2018

Abstract

The present study focuses on the emergency response measures for landslide dams. This work presents a series of centrifuge model tests conducted on the draining processes of barrier dams that are based on the grain composition of the Tangjiashan landslide dam. The effects of diversion channels with trapezoid, triangular, and compound sections on the discharge, process, and size of the residual dam are discussed. The characteristics of the flow erosion during the process of discharge in the different channels are analyzed based on hydrodynamics. The results suggest that a diversion channel with a compound section has a higher initial discharge efficiency and lower peak flow, and the flow process curve corresponds to a "chunky-type." The draining from this type of a diversion channel could clearly reduce the flood pressure of the river downstream and make the entire process smoother. Thus, the excavation of a diversion channel with a compound section is an efficient and safe method for landslide dam emergency mitigation.

Keywords Landslide dam · Centrifugal tests · Diversion channel · Section form · Emergency measure

Introduction

Landslide dams, presented as a natural blockage of a river by the hill slope-derived mass movement, are rather common events in hilly and mountainous areas worldwide (Davies 2002; Dai et al. 2005; Becker et al. 2007). Intense rainfall, rapid snow melts, volcanic eruptions, and earthquakes are the most common landslide dam trigging factors (Do et al. 2016). As a type of natural rockfill dam, landslide dams are extremely prone to failure, and most of them eventually collapse (Dunning et al. 2006). According to statistics, nearly 90% of landslide dams collapse in a year and result in severe flooding (Kuang 1993). A landslide dam may fail owing to a variety of processes including overtopping, instability of the dam slope or piping, as shown in Fig. 1. However, a previous study showed that overtopping was the main failure mode for landslide dams breaching, which was also the mode in the later stage irrespective of its starting cause (Ermini and Casagli 2003; Zhong et al. 2016).

The catastrophic breach triggered by dam-break floods requires appropriate emergency methods to prevent the disastrous consequences for residents located downstream. Tacconi et al. (2016) collectively reviewed approximately 300 landslide dam events that occurred in Italy. Bonnard (2011) reviewed the measures for preventing potential catastrophes caused by a landslide dam-break and concluded that the best approach was to excavate a diversion channel, which could be traced back to 500 years ago when the villagers of Servoz, Monte Blanc, France, excavated a channel to drain a lake at Massif de Plate. After the Mayunmarca rockslide, occurred in 1974 in Peru, a 3-m-deep channel was excavated in the dam to drain the impounded lake at a flood discharge of approximately 11,000 m^3/s (Kojan and Hutchinson 1978). In China, a successful intervention occurred in 2008 when the emergency excavations of a 13-m-deep channel through the famous Tangjiashan landslide dam, which was created during 2008 Wenchuan earthquake of the Southwest Sichuan

✉ Changjing Fu
546684412@qq.com

[1] Key Laboratory for Hydraulic and Waterway Engineering of Ministry of Education, Chongqing Jiaotong University, Chongqing 400074, People's Republic of China

[2] Nanjing Hydraulic Research Institute, Key Laboratory of Failure Mechanism and Safety Control Techniques of Earth-rock Dam of the Ministry of Water Resources, Nanjing 210029, People's Republic of China

[3] Department of Geotechnical Engineering, Nanjing Hydraulic Research Institute, Nanjing 210029, People's Republic of China

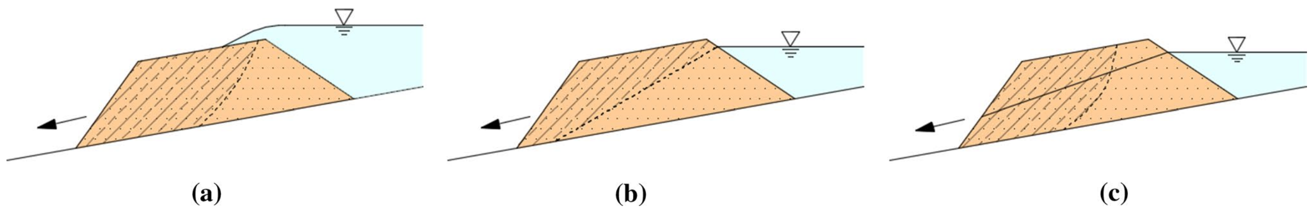

Fig. 1 Failure modes of landslide dam. **a** Overtopping, **b** instability of slope, **c** piping

Province of China, reduced a dam breach from an estimated potential flow of 46,000 m^3/s to a measured peak flow of 6500 m^3/s (Yin et al. 2009; Xu et al. 2009).

Much efforts have been expended to understand the mechanism of a dam-break including soil erosion and open channel hydraulics. Some examples are the National Dam Safety Program (NDSP) project conducted by the Federal Emergency Management Agency (FEMA), USA (Corns 2010), CADAM Project that is a concerted action project funded under the EC FP4 program (Morris 2000), IMPACT project conducted by the European Community during 2001–2003, and FLOODsite project that is also a European Commission funded integrated project conducted in 2004 (Morris and Hassan 2005; Bruijn et al. 2009). For the emergency mitigation work at landslide dams, however, it is still not clear which type of diversion channel, or section form, should be adopted.

Diversion channel excavation, as a common method in emergency risk elimination of barrier dams, could reduce the volume and head of the released water during dam breaching and create a controlled flood. Therefore, in the present study, the authors focus on the impact of the diversion channel section type on the landslide dam draining effect. Given the advantage of simulating a prototype stress, centrifugal model tests are conducted to simulate the draining process of a landslide dam. The effect of three types of channel sections, namely, trapezoidal, triangular, and triangle–trapezoid compound, on the landslide dam breaching process is studied. To better understand the process caused by soil erosion, a hydrodynamic analysis is performed, and the velocity distributions in different channel sections are used to verify the conclusions.

Test materials and method

A model test is an important method for studying the dam-break of an earth-rock dam. Model tests of the landslide dam draining process are performed based on the dam-break centrifugal model test system of the Nanjing Hydraulic Research Institute (NHRI). The main equipment of the system is a 400-gt large-scale geotechnical centrifuge (as shown in Fig. 2), with performance indicators that are listed in Table 1. The test system is equipped with a special model box, whose internal effective size is 1.2 × 0.4 × 0.8 m^3.

Fig. 2 Geotechnical centrifuge (NH-400 gt)

Table 1 Performance indicators of geotechnical centrifuge (NH-400 gt)

Performance index	Value
Capacity	400 gt
Maximum acceleration	200 g
Maximum load	2 t
Effective radius	5 m
Maximum radius	5.5 m

Test materials

The landslide dam materials have the characteristics of a wide grading range, strong heterogeneity, and loose nature, which are highly different from those of artificial dams (Beth et al. 2007). Considering the wide grading of a landslide dam material, the grading curves from five boreholes of the Tangjiashan landslide dam are referenced during the preparation of the model dam material (Chen et al. 2014; Liu et al. 2010). After grain size averaging, the maximum particle size of the test material is controlled at 20 mm. According to the average grading curve of the Tangjiashan landslide dam, an equivalent substitution method is adopted to replace the particle sizes larger than 20 mm with that of 0.075–20 mm. The grading curve of the model dam material is shown in Fig. 3.

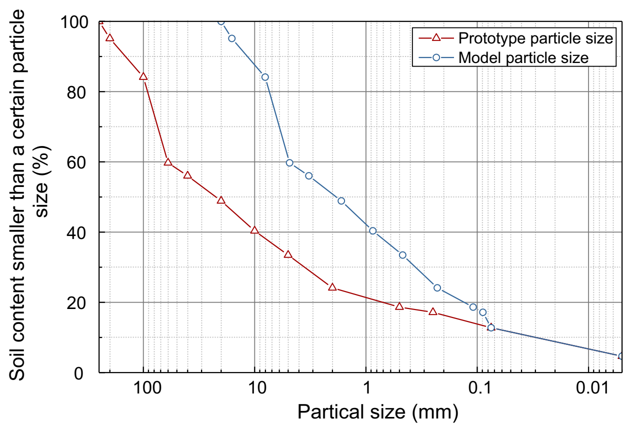

Fig. 3 Gradation of model dam and the Tangjiashan landslide dam

According to the gradation of the model dam material, the content of each grain group could be easily obtained. After sifting, weighting, and stirring, the model dam material is ready for the model dam construction. The basic parameters of the model dam material are presented in Table 2.

Model preparation

The centrifugal model test system is equipped with a special model box, and the model dam is constructed in the box, as shown in Fig. 4. The angle of the downstream slope has a major impact on the process of break flow and breach development, and so, the design of the model dam should satisfy the requirement that the downstream slope angle be small enough similar to the real situation. According to the internal dimensions of the test box, the downstream slope ratio is 1:3.5, which is the average downstream slope ratio of the Tangjiashan landslide dam, whereas the upstream slope ratio is 2:1. The top width and height of the model dam are both 20 cm each. From Fig. 5, it can be seen that the rectangular sharp crested weir, which is 20 cm in height, is extremely high to release the tail water. The washed geo-material of the model dam would accumulate downstream and prevent further failure development in the test. Therefore, the bottom of the test box is raised by 15 cm using compacted clay and a waterproof board with a thickness of 13 and 2 cm, respectively. The clay consists of particles in sizes of 0.075–20 mm and < 0.075 mm, and the mass contents of the two particle groups are both 50%. To ensure that the waterproof board does not settle during the test, the cushion is compacted before placing the board. The tail water, which is 5 cm in depth, is used for the weir flow calculation in the downstream of the model dam. The design of the model dam is shown in Fig. 5.

Table 2 Parameters of model dam material

Index	Median diameter (d_{50}, mm)	Restricted particle diameter (d_{60}, mm)	Dry density (ρ_d, g/cm^3)	Porosity (n, 1)
Value	1.7	4.9	1.59	0.4

Testing method

In landslide dam emergency mitigation research, the objective of the optimization of the diversion channel is to design a section form with a minimum excavation and peak flow and maximum initial flow and capacity of the notch cutting (Chen et al. 2015). In actual projects, a diversion channel with section form of a converse trapezoid is often adopted, such as in the Tangjiashan landslide dam (Liu et al. 2009) and the Karli and Tung Barrier Lakes created by the Pakistan 2005 earthquake of magnitude 7.6 (Schneider. 2008). We understand that the section form of triangle is a special case of the trapezoid form, and the bottom width of the diversion channel would influence the draining process. Accordingly, centrifugal tests for the draining process of a landslide dam with three types of initial channel sections, namely, trapezoidal, triangular, and compound trapezoid–triangle, are performed. The details are shown in Fig. 6, from which it can be noted that the three types of initial channel sections have the same area, implying that they have the same earth excavation quantity.

After the construction of the model dam, according to the cross-section size shown in Fig. 6, the initial diversion channel is excavated through the model dam as shown in Fig. 7. During model testing, the centrifugal acceleration is set to 30 g to simulate the draining process of a 6-m-high landslide dam. According to the inflow of the Tangjiashan barrier lake, the water supply in this test is set to 0.02 m^3/s.

Fig. 4 The basket of the centrifuge and the test box

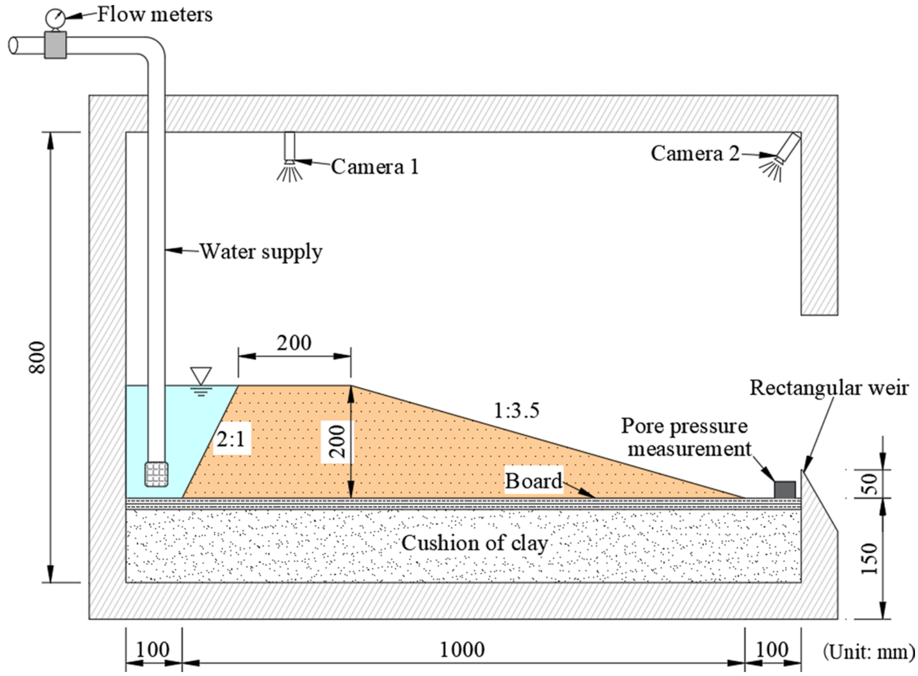

Fig. 5 Overall layout inside the test box

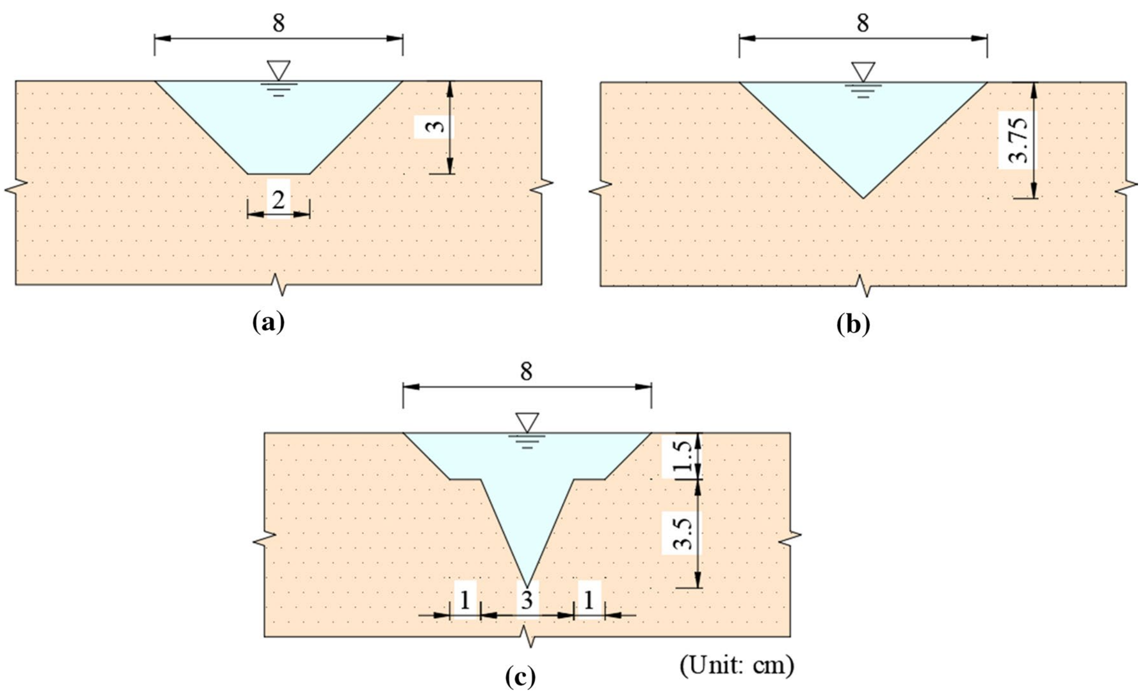

Fig. 6 Design of initial diversion channel. **a** Trapezoid, **b** triangle, **c** compound

Data acquisition

The flux of the breach flow is a critical parameter to study the breaching mechanism of a landslide dam; hence, it is necessary to measure this parameter accurately (Lobovsky et al. 2013). In the past, a flowmeter was usually placed on the drainage outlet of the model box to monitor the export flow. However, as the diameter of circular outlet was extremely large, the tube could not be filled with water. In addition, the drainage water always carried a large number of fine particles that could easily block the pressure-sensitive elements. Therefore, the flux measured by the flowmeter was strongly distorted.

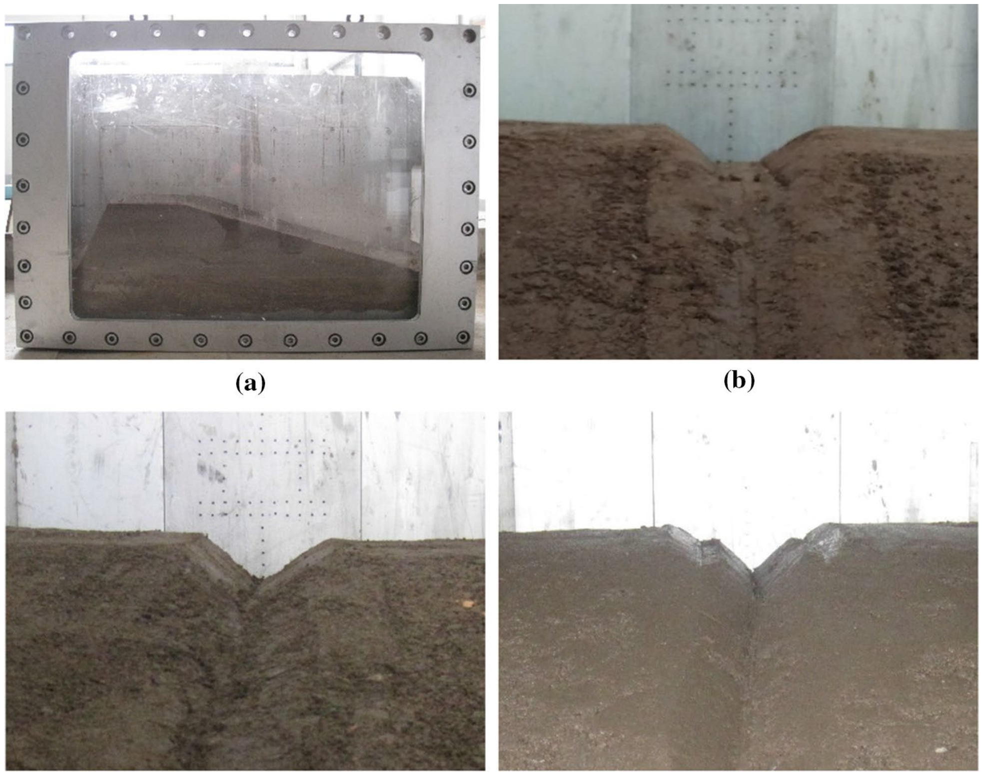

Fig. 7 The model dam and the three types of initial breaches. **a** Profile of the model dam, **b** trapezoidal diversion channel, **c** triangular diversion channel, **d** compound diversion channel

In this work, the downstream side of the test box is designed to be a rectangular sharp crested weir, which is used to monitor the water flow. There are two pore pressure meters embedded in the dam heel to measure the water depth in front of the weir. Under the condition of Ng centrifugal acceleration, the flux process of the dam-break flow can be inverted from the water depth in front of the weir by using the following equation (Zhao et al. 2016):

$$Q = \frac{2}{3}\sigma_c \sigma_f L \sqrt{2NgH}^{\frac{3}{2}} \quad (1)$$

where L is the width of the weir, g is the gravitational acceleration; H is the water head before the weir without near velocity; σ_c and σ_f are, respectively, the lateral contraction coefficient and flux coefficient, and these two coefficients could be calculated by the Belezinski formula (Andrea et al. 2017) as follows:

$$\begin{cases} \sigma_f = 0.32 + 0.01\frac{3-\frac{P}{H}}{0.46+0.75\frac{P}{H}}, \quad 0 < \frac{P}{H} < 3.0 \\ \sigma_f = 0.32, \quad \frac{P}{H} \geq 3.0 \\ \sigma_c = 1 - \frac{0.19\left(1-\frac{L}{B}\right)}{\sqrt[3]{0.2+\frac{P}{H}}}\sqrt[4]{\frac{L}{B}} \end{cases} \quad (2)$$

where P is the height of the rectangular weir and B is the inside net width of the test box. Every parameter is known, except water head H before the weir, and H could be obtained from the two pore pressure meters. Furthermore, the data acquisition of the pore pressure relies on the Isolated Measurement Pods (IMP) data acquisition module and Industrial Personal Computer (IPC). Eight IMP collection modules are used to provide 80 data acquisition channels, and real-time data monitoring could be achieved through the computer.

Test results

Through a series of centrifugal tests, the status of the diversion channel and the flood in the channel could be acquired. In particular, the elapsed time and breach flow are analyzed on the prototype scale according to the centrifugal acceleration (30 g).

Draining process

The draining processes of the channels with three different cross-section types are shown in Fig. 8, and the elapsed

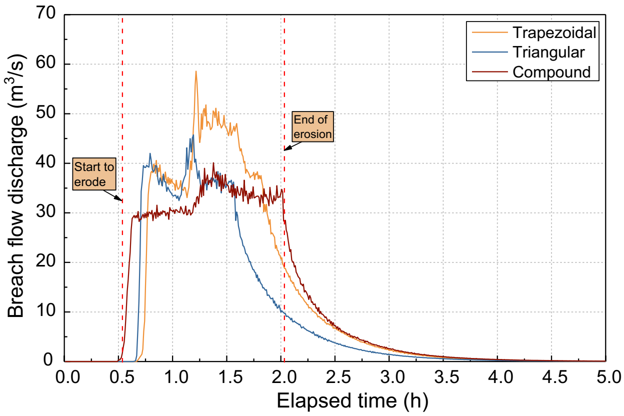

Fig. 8 The breach flow process of different section forms

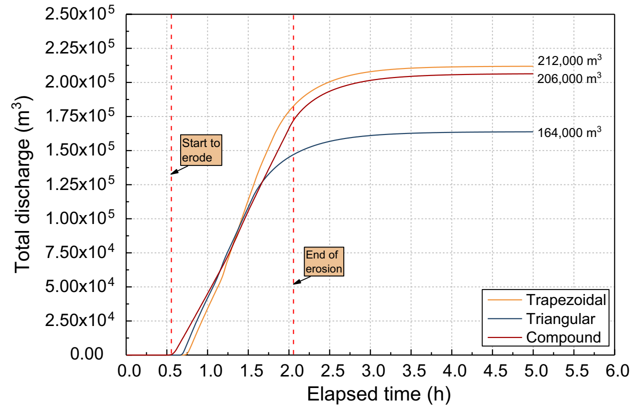

Fig. 9 Total discharge process of different section forms

time, in the figure, starts from the supply of water in the reservoir. As can be seen from the figure, the flux of the three channels is small at the beginning, and maintained at approximately 1.5 m^3/s. When the discharge starts 0.50 h later, the flow rate of the compound channel increases sharply, and the growth rate is 0.076 m^3/s^2. Approximately 0.62 h later, the growth rate of the flow in the compound groove slows down. Then, the flux of the triangular channel increases. The growth rate, which is approximately 0.20 m^3/s^2 in magnitude, is much faster than that of the compound channel. Concurrently, the flow of the trapezoidal channel also starts to increase significantly. However, the difference is that the trapezoidal channel flow growth is not as rapid as that of the triangular and compound channels in the beginning, and the value is approximately 0.0063 m^3/s^2. The reason for this phenomenon is that the bottom elevation of the three groove types, i.e., trapezoidal, triangular, and compound trapezoid–triangle, is reduced in turn, and the water head increases successively. Thus, the flow of the compound and triangular channel increases in a shorter time, and the flow of the trapezoidal channel, in contrast, grows slowly. Approximately 1.19 h later, the flow of the triangular channel reaches its peak, which is approximately 45.7 m^3/s. The peak time and flux of the trapezoidal channel are 1.21 h and 58.6 m^3/s, respectively, and the same for the compound channel are 1.38 h and 40.1 m^3/s, respectively. Subsequently, the downstream slopes of the model dams become coarse, and the times when the flow of the trapezoidal, triangular, and compound trapezoid–triangle channel begins to decrease are 1.8 h, 1.6 h, and 2.0 h, respectively.

Total discharge process

It is known that if the elapsed time is on the x-axis and the flux of the breach flow is on the y-axis, the total charge until elapsed time t is the area enclosed by the curve of the breach flow process and lines of $y = 0$ and $x = t$. Thus, according to Fig. 8, the total discharge process of the different section forms could be obtained as shown in Fig. 9. The rules for the total discharge process are similar to those of the breach flow process. Approximately 0.55 h later, starting from the supply of water in the reservoir, the dam begins to be scoured, and simultaneously, the discharge of the compound channel increases sharply. This implies that the channel with a compound section could discharge the water at a relatively high speed in the initial stage and release the reservoir water at an earlier time. Subsequently, the triangular and trapezoidal channels begin to release water in turn. According to the three curves between the time of start and end of the erosion in Fig. 9, it can be seen that the slopes of the trapezoidal, triangular, and compound channel decrease in turn. It is indicated that draining process of the trapezoidal channel is rapid and that of the compound channel is much gentler than of the other two. The compound channel reaches a relatively larger total discharge, approximately 206,000 m^3 in value and that of the trapezoidal and triangular channels is 212,000 and 164,000 m^3, respectively.

Breach remaining

The breaches remaining with the three different sections are shown in Fig. 10. It is important to note that all the three diversion channels are excavated in the middle of the dam crest. However, the erosion intensity, during the process of overtopping, is high on the right side of the breach, which results in a residual breach located near the right dam abutment. The reason for this phenomenon is that downstream of the model is placed in the basket near the center side of the centrifuge, which can also be seen in Fig. 4. When the basket rotates in a clockwise direction, it provides a small acceleration to the model, which points to the left of the dam. The value of the acceleration being small, the accuracy of the test results will not be significantly affected. From Fig. 10, it can be seen that the shape of all the breaches with

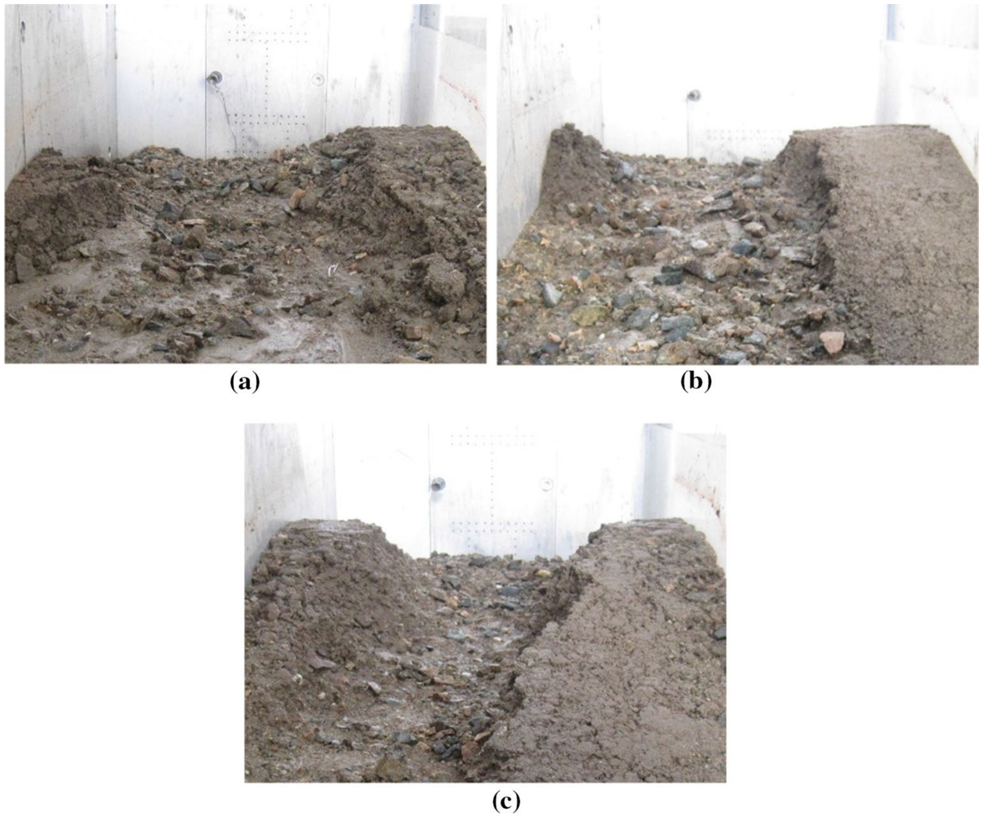

Fig. 10 Breach remaining of three drainage channels with different section forms. **a** Trapezoidal diversion channel, **b** triangular diversion channel, **c** compound diversion channel

different initial section types is an "inverted trapezoid," and the final width of the breach is larger than the final depth of the breach. [The relationship between the final width and depth of the breach can be found in ref. (Zhang et al. 2009; Morris et al. 2002).] Specific sizes of the breaches remaining are shown in Table 3.

From Table 3, the same conclusion can be obtained. The trapezoidal channel has the largest peak flow and the most intense erosion, and the width expansion of the trapezoidal channel is larger than of the other two. The triangular channel has the largest depth cutting distance. The compound channel has the lowest peak flow, and accordingly, the erosion strength on it is small. Thus, the width expansion of the compound channel is small. Owing to the section shape of the compound channel, it has a relatively large depth cutting distance, and it releases more water in the reservoir.

According to the draining processes, and the total discharges and sizes of the breaches remaining with different initial sections, it is indicated that channel with a compound section has a relatively larger total discharge with a lower peak flow, and its flow curve can be named as "chunky-type." Compared with the other two types, the discharge process of the channel with the compound section is more rapid and safe.

Table 3 Sizes of breach with three section types discharge channels

Section type	Size of breach remaining			Breach extended distance		
	Top width (m)	Bottom width (m)	Depth (m)	Top width (m)	Bottom width (m)	Depth (m)
Trapezoidal	9.3	8.1	1.6	6.9	7.5	0.7
Triangular	7.5	4.8	2.4	5.1	4.8	1.275
Compound	6.3	2.4	2.7	3.9	2.4	1.2

Hydrodynamic analysis

Three channels have the same initial top width, i.e., 2.4 m. According to Table 3, the top width of the trapezoidal channel is the largest, followed by those of the triangular and compound channels. From the theory of open channel hydrodynamics (Han and Easa 2016; Abrari et al. 2016), the flow velocity at the bottom of the trapezoidal channel is approximately the same as that of the flow on the bilateral walls. It is known that the flow velocity of the water flow is positively related to the scouring capacity; therefore, rates of width expansion and vertical cutting of the trapezoidal channel are almost similar at the initial draining stage. However, as the boundary layer velocity is slow at the bottom of the trapezoidal channel, the erosion of the depth cutting is weak. Therefore, the breach remaining in the trapezoidal channel is shallow in depth and large in the top and bottom widths. For the triangular channel, the flow velocity at the bottom is much faster than that on the bilateral walls, so that the erosion at the bottom is stronger than that on the sidewalls; therefore, a channel of this type has a faster notch cutting. The breach remaining in the triangular channel is narrow in width and deeper than that of the trapezoidal channel. The flow velocity distribution of the compound channel is similar to that of the triangular channel. However, the compound channel has a faster flow at the bottom and slower at the sidewalls. Thus, the compound channel has the strongest erosion in the depth direction, and accordingly, the maximum depth of the breach remaining in the channel.

From the law of soil erosion, the lower parts of the triangular and compound channels are all triangle shaped, and they have smaller areas of interaction between the soil and water at the same flow depth, implying that they have smaller wetted perimeters χ. Therefore, the shape of the channel in the lower part strengthens its erosion, and these two types of draining channels achieve the objective of rapidly decreasing the reservoir water. However, the notch cutting and width expansion of the triangular channel is extremely fast, resulting in a large water head difference. Thus, the triangular channel has a higher peak flow, and the discharge process is difficult to control. In comparison, the notch cutting of the compound channel is fast at the beginning, which is beneficial for improving the discharge efficiency and decreasing the reservoir water in the initial stage of the discharge. The upper part of the compound channel, in the shape of a trapezoid, has an obvious effect on preventing the horizontal expansion. The width expansion of the compound channel could be limited to a lower speed, and the peak flow could be decreased further. Thus, the breach remaining in the compound channel has a smaller width expansion and larger cutting depth after draining.

Concluding remarks

The section type of a landslide dam diversion channel has a major effect on the draining process and total discharge. Based on the grading curve of the Tangjiashan landslide dam, centrifugal model tests on the draining efficiency of the diversion channels with trapezoidal, triangular, and compound sections are conducted. The test results prove that the diversion channel with a compound section could release water rapidly with a lower peak flow and reach a higher total discharge. The curve of the draining process is of the "chunky-type." During a landslide dam emergency drainage, a diversion channel with a compound section could improve the efficiency at the initial stage, lower the peak flow, and reduce the flood pressure of the river channel downstream. Owing to the larger total discharge after draining, the diversion channel with a compound section could lower the water level rapidly to the maximum. Therefore, the excavation of a diversion channel with a compound section is an efficient and safe method in the emergency risk elimination of barrier dams.

Acknowledgements The authors gratefully acknowledge the financial support from the National Natural Science Foundation of China under Grant No. 51709025, the special funding for post doctoral research projects of Chongqing under Grant No. Xm2017092, the National Engineering Research Center for Inland Waterway Regulation and Key Laboratory for Hydraulic and Waterway Engineering of Ministry of Education Open Foundation under Grant No. SLK2015B09, the National Science and Technology Support Program of China under Grant No. 2015BAK09B01, the basic science and advanced technology research projects of Chongqing under Grant No. cstc2016jcyjA0551, and the science and technology project of Chongqing Municipal Education Commission under Grant No. KJ1600516, respectively.

References

Abrari E, Beirami MK, Ergil M (2016) Prediction of the discharges within exponential and generalized trapezoidal channel cross-sections using three velocity points. Flow Meas Instrum 54:27–38

Andrea M, Marco P, Massimo T (2017) Experimental and numerical analysis of side weir flows in a converging channel. J Hydraul Eng 143(7):04017009-1–04017009-15

Becker JS, Johnson DM, Paton D (2007) Response to landslide dam failure emergencies: issues resulting from the October 1999 Mount Adams landslide and dam-break flood in the Poerua River, Westland, New Zealand. Nat Hazards Rev 2(8):35–42

Beth PS, Michelle G, Burbank DW, Michael O, Arjun H, Emmanuel G (2007) Bedload-to-suspended load ratio and rapid bedrock incision from Himalayan Landslide-dam lake record. Quat Res 68(1):111–120

Bonnard C (2011) Technical and human aspects of historic rockslide-dammed lakes and landslide dam breaches. Springer, Berlin

Bruijn KD, Klijn F, Ölfert A, Penningrowsell E, Simm J, Wallis M (2009) Flood risk assessment and flood risk management. An introduction and guidance based on experiences and findings of FLOODsite (an EU-funded Integrated Project). Deltares

Chen Z, Ma L, Yu S, Chen S, Zhou X, Sun P, Li X (2014) Back analysis of the draining process of the Tangjiashan Barrier Lake. J Hydraul Eng 141:05014011-1–05014011-14

Chen S, Lin T, Chen C (2015) Modeling of natural dam failure modes and downstream riverbed morphological changes with different dam materials in a flume test. Eng Geol 188:148–158

Corns CF (2010) Status report on the National Dam Safety Program. Paper read at Safety of Small Dams, pp 4–7

Dai FC, Lee CF, Deng JH, Tham LG (2005) The 1786 earthquake-triggered landslide dam and subsequent dam-break flood on the Dadu River, southwestern China. Geomorphology 65(3–4):205–221

Davies TR (2002) Landslide-dambreak floods at Franz Josef Glacier township, Westland, New Zealand: a risk assessment. J Hydrol (N Z) 41(1):1–17

Do XK, Kim M, Nguyen HPT, Jung K (2016) Analysis of landslide dam failure caused by overtopping. Procedia Eng 154:990–994

Dunning SA, Rosser NJ, Petley DN, Massey CR (2006) Formation and failure of the Tsatichhu landslide dam, Bhutan. Landslides 3(2):107–113

Ermini L, Casagli N (2003) Prediction of the behaviour of landslide dams using a geomorphological dimensionless index. Earth Surf Proc Land 28(1):31–47

Han YC, Easa SM (2016) Superior cubic channel section and analytical solution of best hydraulic properties. Flow Meas Instrum 50:169–177

Kojan E, Hutchinson JN (1978) Chapter 9—Mayunmarca rockslide and debris flow, Peru. Dev Geotech Eng 14:315–353

Kuang S (1993) Formation mechanisms and prediction models of debris flow due to natural dam failures. J Sedim Res 4:42–57

Liu N, Zhang J, Lin W, Chen W, Chen Z (2009) Draining Tangjiashan barrier lake after Wenchuan earthquake and the flood propagation after the dam break. Sci China Ser E-Tech Sci 52(4):801–809

Liu N, Chen Z, Zhang J, Lin W, Chen W, Xu W (2010) Draining the Tangjiashan barrier lake. J Hydraul Eng 136(11):914–923

Lobovsky L, Botia-Vera E, Castellana F, Mas-Soler J, Souto-Iglesias A (2013) Experimental investigation of dynamic pressure loads during dam break. J Fluids Struct 48:407–434

Morris MW (2000) CADAM: concerted action on dambreak modelling. Oxford, Hr Wallingford Limited

Morris MW, Hassan M (2005) IMPACT: investigation of extreme flood processes and uncertainty—a European research project

Morris MW, Hassan M, Vaskinn KA (2002) Conclusions and recommendations from the IMPACT project WP2: Breach formation. HR Wallingford Ltd., Oxford

Schneider JF (2008) Seismically reactivated Hattian slide in Kashmir, Northern Pakistan. J Seismol 13(3):387–398

Tacconi C, Segoni S, Casagli N, Catani F (2016) Geomorphic indexing of landslide dams evolution. Eng Geol 208:1–10

Xu Q, Fan X, Huang R, Westen CV (2009) Landslide dams triggered by the Wenchuan Earthquake, Sichuan Province, south west China. Bull Eng Geol Environ 68(3):373–386

Yin Y, Wang F, Sun P (2009) Landslide hazards triggered by the 2008 Wenchuan earthquake, Sichuan, China. Landslides 6(2):139–152

Zhang J, Li Y, Xuan G, Wang X, Li J (2009) Overtopping breaching of cohesive homogeneous earth dam with different cohesive strength. Sci China Ser E Technol Sci 52(10):3024–3029

Zhao T, Chen S, Wang J, Zhong Q, Fu C (2016) Centrifugal model tests overtopping failure of barrier dams. Chin J Geotech Eng 38(11):1965–1972

Zhong Q, Wu W, Chen S, Wang M (2016) Comparison of simplified physically based dam breach models. Nat Hazards 84(2):1–34